JPL Publication 91-11

Theoretical Prediction of the Impact of Auger Recombination on Charge Collection From an Ion Track

Larry D. Edmonds

March 1, 1991

NASA
National Aeronautics and
Space Administration

Jet Propulsion Laboratory
California Institute of Technology
Pasadena, California

JPL Publication 91-11

Theoretical Prediction of the Impact of Auger Recombination on Charge Collection From an Ion Track

Larry D. Edmonds

March 1, 1991

National Aeronautics and
Space Administration

Jet Propulsion Laboratory
California Institute of Technology
Pasadena, California

The research described in this publication was carried out by the Jet Propulsion Laboratory, California Institute of Technology, under a contract with the National Aeronautics and Space Administration (NASA) under the NASA Microelectronics Radiation Effects Ground Test Program.

ABSTRACT

A recombination mechanism that significantly reduces charge collection from very dense ion tracks in silicon devices was postulated by Zoutendyk et al. The theoretical analysis presented here concludes that Auger recombination is such a mechanism and is of marginal importance for tracks produced by 270-MeV krypton, but of major importance for higher density tracks. The analysis shows that recombination loss is profoundly affected by track diffusion. As the track diffuses, the density and recombination rate decrease so fast that the linear density (number of electron-hole pairs per unit length) approaches a non-zero limiting value as $t \rightarrow \infty$. Furthermore, the linear density is very nearly equal to this limiting value in a few picoseconds or less. When Auger recombination accompanies charge transport processes that have much longer time scales, it can be simulated by assigning a reduced linear energy transfer to the ion.

CONTENTS

1. INTRODUCTION

Zoutendyk et al. [1] postulated the existence of a recombination mechanism that significantly reduces charge collection from very dense ion tracks in silicon devices. This can impact device susceptibility to single-event effects (SEE). It is reasonable to ask if Auger recombination (AR) can have such an effect. This report presents a theoretical investigation of the impact of AR on charge collection from an ion track.

2. PHYSICAL MODELS

Ion tracks consist of high electron-hole pair (EHP) density, which is well described by the ambipolar diffusion equation

$$D \text{ div grad } P - \delta P/\delta t = R \qquad (1)$$

where D is the ambipolar diffusion constant and P is the excess hole density (hole density minus equilibrium hole density). Because of quasi-neutrality and high carrier density, P is also equal to the EHP density. R is the recombination rate and $\delta/\delta t$ denotes partial derivative with respect to time. It will be seen that the time scale for significant AR is a few picoseconds or less, which is very short compared to typical lifetimes for Shockley-Read-Hall recombination (SRHR). Therefore, SRHR has a negligible effect on EHP loss via AR, and the objective is to

estimate only this loss, so only AR is considered in this analysis. For quasi-neutral and high-density conditions, the AR rate used by the numerical simulation code PISCES [2] reduces to

$$R = CP^3$$

where $C=C_n+C_p$ with $C_n=2.8\text{x}10^{-31}$ cm^6/s and $C_p=9.9\text{x}10^{-32}$ cm^6/s (default values used by PISCES). Therefore, the governing equations are

$$D \text{ div grad } P - \delta P/\delta t = CP^3 \quad \text{for } t > 0 \tag{2}$$

$$P = P_I \quad \text{for } t = 0 \tag{3}$$

where P_I is the initial EHP density. The track is treated as infinitely long and uniform in the vertical (z) coordinate so that P(r,t) depends only on the radial distance r (where $r^2=x^2+y^2$) and on time t. The objective is to obtain an estimate of P and of the linear density (number of EHPs per unit length), which is the x and y integral of P.

3. MATHEMATICAL ANALYSIS

The first objective is to solve (2) and (3) for P. These equations will be converted into an integral equation, but the proofs of some theorems to follow require the integral equation to be

solvable by iteration (i.e., iteration produces a converging sequence of iterates). To accomplish this, (2) will be rewritten so that the right side has a bounded P derivative. Define P_M by

$$P_M \equiv \max_r P_I(r). \tag{4}$$

It is evident that $P(r,t) \leq P_M$ for all r,t and, therefore, the solution P is not changed if (2) is replaced with

$$D \text{ div grad } P - \delta P/\delta t = CF(P) \tag{5}$$

where F is defined by

$$F(\tau) \equiv \begin{cases} \tau^3 & \text{if } |\tau| \leq P_M \\ P_M^2\, \tau & \text{if } |\tau| > P_M. \end{cases} \tag{6}$$

Although the right side of (5) is indistinguishable from the right side of (2) when P is the correct solution, there can be a difference in the equations when iteration is used to solve them because some initial guesses can cause the equations to produce different sequences of iterates. The motivation for (5) is to make convergence proofs easier.

(A) Integral Equations

Define the constant B by

$$B \equiv 3CP_M^2 \tag{7}$$

and write (5) as

$$\text{div grad } P - D^{-1}(BP + \delta P/\delta t) = D^{-1}[CF(P) - BP]. \qquad (8)$$

Define P_0 as the solution to

$$\text{div grad } P_0 - D^{-1}\delta P_0/\delta t = 0 \quad \text{for } t > 0 \qquad (9)$$

$$P_0 = P_I \quad \text{for } t = 0 \qquad (10)$$

and define P_B by

$$P_B \equiv e^{-Bt} P_0 \qquad (11)$$

so that P_B satisfies

$$\text{div grad } P_B - D^{-1}(BP_B + \delta P_B/\delta t) = 0 \quad \text{for } t > 0 \qquad (12)$$

$$P_B = P_I \quad \text{for } t = 0. \qquad (13)$$

The two-dimensional infinite-space Green's function for the operator on the left of (9) is [3]

$$G(X,t;X',t') = (t-t')^{-1} \exp[-\{(x-x')^2+(y-y')^2\}/\{4D(t-t')\}] \qquad (14)$$

where uppercase X denotes the vector (or point in space) with components x and y. G can be used to solve (9) and (10) for P_0 with the result [3]

$$P_0 = (4\pi D)^{-1} \int P_I(r')\ G(X,t;X',0)\ d^2X' \qquad (15)$$

where the integral is defined by

$$\int d^2X' \equiv \int_{-\infty}^{\infty} \int_{-\infty}^{\infty} dx'\ dy'. \qquad (16)$$

The B on the left of (8) can be eliminated by a change in variables produced by multiplying P by e^{Bt} and the equation can then be inverted by using G [3]. The final result is

$$P = P_B + (4\pi D)^{-1} \int_0^t \int [BP - CF(P)]\ e^{-B(t-t')} G\ d^2X'\ dt'. \qquad (17)$$

For notational brevity, the arguments of P and G in the integrand are not displayed, but P in the integrand is P(r',t') and G is G(X,t;X',t'). The analysis leading to (17) also applies if B is replaced with zero and the result is

$$P = P_0 - C(4\pi D)^{-1} \int_0^t \int F(P)\ G\ d^2X'\ dt'. \qquad (18)$$

(B) Bounds by Iteration

The method used in later sections to estimate P and the linear density will consist of constructing lower and upper bounds. Some concepts, discussed in this section, will be needed for future use.

We will call a function P_1 an upper bound for another function P_2 if

$$P_1(r,t) \geq P_2(r,t) \quad \text{for all } r,t \geq 0. \tag{19}$$

P_1 is called a lower bound for P_2 if and only if P_2 is an upper bound for P_1.

Let $P^{(2)}$ be obtained by starting with some $P^{(1)}$ (parentheses emphasize that the superscripts are not exponents) and iterating (17); i.e., they are related by

$$P^{(2)} = P_B+(4\pi D)^{-1}\int_0^t \int [BP^{(1)}-CF(P^{(1)})]\, e^{-B(t-t')}G\, d^2X'\, dt'. \tag{20}$$

It is easy to show that $B\tau-CF(\tau)$ is an increasing function of τ and, therefore, if $P^{(1)}$ is an upper bound for P, the right side of (20) is an upper bound for the right side of (17), i.e., $P^{(2)}$ (the left side of (20)) is an upper bound for P (the left side of (17)). Therefore, if we iterate (17) by starting with an upper bound for P, another upper bound is obtained. Repeated iteration

produces a sequence of upper bounds. Similarly, lower bounds produce new lower bounds. Equation (18) has a similar property except that the negative sign in front of the integral causes upper bounds to produce lower bounds and vice versa. It is shown in Appendix A that a sequence of functions obtained by iterating (17) converges, and if $P^{(1)}$ and $P^{(2)}$ are related by (20), then $P^{(2)}$ will be a better estimate of P than $P^{(1)}$ is (unless $P^{(1)}=P$, in which case $P^{(2)}=P$)[1]. Equation (18) does not have this property and iteration typically produces a wild oscillation (in the sense that if the initial function is a little larger than P, the first iterate will be much smaller than P and the second iterate will be much much larger than P, etc.). However, (18) will produce a good (accurate) bound if we start with a sufficiently good bound.

The convergence proof (Appendix A) applies only for finite t. Functions produced by iteration of (17) have an unfortunate property in the limit as $t\to\infty$. This can be seen by integrating (20) while using

$$\int G \, d^2X = 4\pi D \tag{21}$$

to get

---

1. As an incidental point, if B was $3CP_M^2/2$ instead of $3CP_M^2$, the iteration would converge faster. But (18) would lose the property of bounds producing new bounds. Without this property, the only simple error estimates available are those derivable from Banach's fixed point theorem, which are extremely pessimistic.

$$\int P_2 \, d^2X = \int P_B \, d^2X + \int_0^t \left[\int (BP_1 - CP_1^3) \, d^2X' \right] e^{-B(t-t')} \, dt'.$$

For large t, the first integral on the right goes to zero and, because of the exponential coefficient, only the asymptotic (in t') value of

$$\int (BP_1 - CP_1^3) \, d^2X'$$

contributes to the t' integral. Assuming that the P_1^3 integral goes to zero, we have

$$\lim_{t\to\infty} \int P_2 \, d^2X = \left[\lim_{t'\to\infty} \int (BP_1 - CP_1^3) \, d^2X' \right] \int_0^t e^{-B(t-t')} \, dt'$$

$$= \lim_{t\to\infty} \int P_1 \, d^2X.$$

Therefore, if we define the linear densities $N_1(t)$ and $N_2(t)$ by

$$N_i(t) = \int P_i \, d^2X \quad \text{for } i = 1,2$$

we conclude that N_2 has the same limiting value as N_1. In a sequence of iterates obtained by iterating (17), each function produces the same limiting value for the linear density as the initial guess. Fortunately, this problem is not too serious when

working with upper bounds for P. The reason is that if we start with an upper bound $P^{(0)}$ and then iterate (17) n times to obtain an upper bound $P^{(n)}$, we will find that the linear density $N^{(n)}$ first decreases and then increases in t. But the actual linear density is strictly decreasing so an upper bound at a given time is also an upper bound for all later times. Therefore, $N^{(n)}$ must be plotted in t only until it begins to increase. The minimum value can be used for all later times.

The above statements indicate that the following methods will be effective for constructing bounds for the linear density:

(i) To obtain an upper bound:

1: Start with an upper bound $P^{(0)}$ for P and iterate (17) n times to obtain an upper bound $P^{(n)}$ with corresponding linear density $N^{(n)}(t)$. Plot $N^{(n)}$ against t until it reaches a minimum and use the minimum value for all later times

or

2: Start with a lower bound $P^{(0)}$ for P and iterate (17) n times to obtain a lower bound $P^{(n)}$. Then iterate (18) once to obtain an upper bound $P^{(n+1)}$.

(ii) To obtain a lower bound:

1: Start with a lower bound $P^{(0)}$ for P and be content with it (iterating (17) will not improve the limiting value of the linear density)

or

2: Start with an upper bound $P^{(0)}$ for P and iterate (17) n times to obtain an upper bound $P^{(n)}$. Then iterate (18) once to obtain a lower bound $P^{(n+1)}$.

(C) An Initial Estimate

P can be estimated by constructing upper and lower bounds and the previous discussion shows how bounds can be constructed. But those methods require that we start with a bound and another method, discussed here, is needed to construct an initial bound. The idea is to guess at a function and then perform a test to determine if the function is a bound for P. One such test is the following. Let P_E be a bounded and well behaved (in the sense that div grad P_E and $\delta P_E/\delta t$ exist) function that is to be tested. P_E is required to satisfy

$$P_E = P_I \quad \text{at } t = 0. \tag{22}$$

Define g by

$$g \equiv -D \text{ div grad } P_E + \delta P_E/\delta t + CP_E^3 \ . \tag{23}$$

It is shown in Appendix B that:

If $g(r,t) \geq 0$ for all $r,t \geq 0$, then P_E is an upper bound for P. (24)

If $g(r,t) \leq 0$ for all $r,t \geq 0$, then P_E is a lower bound for P. (25)

If neither (24) or (25) are satisfied, the test is inconclusive and we should guess at another P_E and try the test again.

(D) A Particular Estimate when P_I is a Gaussian Function

Consider the special case

$$P_I(r) = N_0(4\pi D t_0)^{-1} \exp[-(4Dt_0)^{-1} r^2] \qquad (26)$$

for some constants N_0 (the initial linear density) and t_0. The form (26) is not a good approximation for an actual ion track but it greatly simplifies the analysis and can produce useful estimates when combined with judicious curve fitting (this is illustrated in the next section). The integral in (15) can be evaluated with the result

$$P_0(r,t) = N_0[4\pi D(t+t_0)]^{-1} \exp\{-[4D(t+t_0)]^{-1} r^2\} . \qquad (27)$$

Define P_{E1} by

$$P_{E1} \equiv [2Ct + (f(t)P_0)^{-2}]^{-1/2} \qquad (28)$$

where f satisfies

$$f(0) = 1 \tag{29}$$

$$f(t) > 0 \quad \text{for all } t > 0 \tag{30}$$

but otherwise remains to be determined.

Using the chain rule to evaluate the derivatives on the right side of (23), we find that several terms subtract out (which is the motivation behind the particular estimate P_{E1}), and the result is

$$g = fP_0(2Ctf^2P_0^2 + 1)^{-5/2}\, g_1 \tag{31}$$

where g_1 is defined by

$$g_1 \equiv (2Ctf^2P_0^2+1)f'/f + [3C/(2D)]t(t+t_0)^{-2}f^2P_0^2r^2 \tag{32}$$

and the prime denotes differentiation. P_{E1} will be constructed to be a lower bound for P by selecting f to make g satisfy (25). This can be accomplished by selecting f to make g_1 satisfy

$$\max_{r\geq 0} g_1(r,t) = 0 \quad \text{for all } t \geq 0. \tag{33}$$

Using (27), we find that the maximum in r is a relative maximum given by

$$\max_{r\geq 0} g_1(r,t) =$$

$$(f'/f)+3C(4\pi D)^{-2}t(t+t_0)^{-3}N_0^2f^2 \exp[(2/3)(t+t_0)(f'/f)-1]$$

so (33) becomes

$$f'/f = -(3/2)Kt(t+t_0)^{-3}f^2 \exp[(2/3)(t+t_0)f'/f] \quad (34)$$

where

$$K \equiv 2CN_0^2e^{-1}(4\pi D)^{-2} . \quad (35)$$

To solve for f, define the function $H^{-1}:[0,\infty)\rightarrow[0,\infty)$ by

$$H^{-1}(u) \equiv ue^u . \quad (36)$$

Note that H^{-1} is strictly increasing so it has an inverse, denoted H, which is also strictly increasing. Equation (34) can be written as

$$f'/f = -(3/2)(t+t_0)^{-1}H(Kt(t+t_0)^{-2}f^2)$$

and integrating while using (29) gives

$$f(t) = \exp\left[-(3/2)\int_0^t (\tau+t_0)^{-1}H(K\tau[\tau+t_0]^{-2}f^2(\tau))\ d\tau\ \right]. \quad (37)$$

Equation (37) can be solved for f by iteration[1].

Iteration of (37) is done numerically, but in numerical work we cannot go to the limit as $t\to\infty$. We must work with a finite interval [0,T] and it is necessary to know how large T must be in order for f(T) to adequately approximate $f(\infty)$. This can be determined by writing

$$f(T)/f(\infty) = \exp\left[(3/2)\int_T^\infty (\tau+t_0)^{-1}H(K\tau[\tau+t_0]^{-2}f^2(\tau))\ d\tau\ \right] .$$

If we require, for example, that the ratio be between 0.99 and 1, then we require

$$(3/2)\int_T^\infty (\tau+t_0)^{-1}H(K\tau[\tau+t_0]^{-2}f^2(\tau))\ d\tau < 0.01 .$$

It is easy to show that $H(u)\le u$ for positive u. Also, $f(\tau)\le 1$ so the above condition will be satisfied if

---

1. A convergence proof is not required because convergence is not used to prove any theorems. Convergence is needed only for the numerical computation of f and can be verified on a case-by-case basis during the computation. But it is useful to note that (37) is similiar to (18) in the sense that upper bounds produce lower bounds and vice versa. If the initial guess is f=1 (an upper bound), iteration will produce a sequence of alternating upper and lower bounds. The correct solution is bracketed between any pair of adjacent iterates and is known to within a given tolerance when the difference between adjacent iterates is less than that tolerance.

$$(3/2)\int_{T}^{\infty} K\tau(\tau+t_0)^{-3}\, d\tau < 0.01$$

or

$$(3/2)K(T+t_0/2)(T+t_0)^{-2} < 0.01 \ .$$

This will be satisfied if

$$T = 150K \ . \tag{38}$$

In addition to evaluating T, the previous analysis also demonstrated that the integral in (37) must be finite, even in the limit as $t\to\infty$. Therefore, we conclude from (37) that $f(\infty)>0$. It is not difficult to show that

$$P_{E1} \to f(t)P_0 \quad \text{as } t \to \infty \tag{39}$$

so that a lower bound $N_{E1}(t)$ for the linear density N(t) satisfies

$$N_{E1}(t) \to f(t)N_0 \quad \text{as } t \to \infty \tag{40}$$

and does not go to zero as $t\to\infty$. The conclusion is that some EHPs never will recombine (via AR) no matter how long we wait. It is not difficult to show that P_{E1} is within 1% of the right side of (39) and, therefore, N_{E1} is within 1% of the right side of (40), when t>T. But f(t) is within 1% of $f(\infty)$ when t>T. Therefore, N_{E1}

is within 2% of its limiting value $f(\infty)N_0$ when t>T. Nearly all AR that ever will occur will do so in a time T given by (38).

With f now regarded as known, a lower bound estimate N_{E1} for the linear density can be evaluated from

$$N_{E1}(t) = \int P_{E1}\, d^2X = 2\pi\int_0^\infty [2Ct+(fP_0)^{-2}]^{-1/2} r\, dr\ . \qquad (41)$$

An upper bound for P is P_{E2} obtained from (18) according to

$$P_{E2} = P_0 - C(4\pi D)^{-1}\int_0^t\int P_{E1}{}^3 G\, d^2X'\, dt' \qquad (42)$$

and an upper bound for the linear density is N_{E2} given by

$$N_{E2}(t) = \int P_{E2}\, d^2X\ . \qquad (43)$$

Integrating (42) while using (21) and (28) gives

$$N_{E2}(t) = N_0 - 2\pi C\int_0^t\int_0^\infty \{2Ct'+[f(t')P_0(r,t')]^{-2}\}^{-3/2}\, rdr\, dt'. \qquad (44)$$

The integrals in (41) and (44) can be evaluated using (27) and the change in variables

$$u = \exp([4D(t+t_0)]^{-1}r^2)$$

with the result

$$N_{E1} = f_1^{-1} \ln[f_2+(1+f_2^2)^{1/2}] \tag{45}$$

$$N_{E2} = N_0-(1/2)\int_0^t f_3(t')\ dt' \tag{46}$$

where

$$f_1 \equiv (2Ct)^{1/2}[4\pi D(t+t_0)]^{-1} \tag{47}$$

$$f_2 \equiv N_0 f_1 f \tag{48}$$

$$f_3 \equiv (tf_1)^{-1}(\ln[f_2+(1+f_2^2)^{1/2}]-f_2(1+f_2^2)^{-1/2}) \ . \tag{49}$$

4. COMPUTER CODE AND NUMERICAL EXAMPLES

A computer code that numerically evaluates the lower and upper bound linear density estimates N_{E1} and N_{E2} is listed in Appendix C. The value used for D is constructed from PISCES default values of 500 and 1000 $cm^2/V\text{-}s$ for hole and electron mobilities, respectively. This gives (at room temperature) D=17.3 cm^2/s. C is constructed from PISCES default values as discussed in section 2. The code assumes the initial density to be given by

$$P_I = N_0(\pi r_c^2)^{-1} \exp(-r^2/r_c^2) \tag{50}$$

where the initial linear density N_0 and characteristic radius r_c are specified by the user. The code output is in a file called RCOM.OUT and is the estimated fractional surviving linear density

$$[(N_{E1}+N_{E2})/2 \pm (N_{E2}-N_{E1})/2]/N_0 \ .$$

Martin et al.[4] give the radial profile for a track produced by 270-MeV (initial energy) Kr at selected depths in a Si target. Their data was used to plot Figures 1, 2, and 3 which refer to depths of 5, 15, and 25 μm respectively. Because the computer code assumes a profile of the form (50), it is necessary to curve fit. This motivates the construction of the upper curves in each figure, which are the integrated densities, i.e., the total number of EHPs contained within a given radius (the asymptotic values of these curves are the linear densities). These curves are useful for telling us where curve fitting is and is not required to be accurate. Accuracy is not needed on intervals containing a negligible fraction of the EHPs. The dashed curves in the figures are the functions of the form (50) that were selected to represent the actual curves. In all cases, the fitting curves produce the same linear densities as the actual curves. The remaining criteria for selecting the fitting curves is a mixture of intuitive judgment and reasoning. For example, in the 25 μm case (Figure 3), the fit is reasonably good from $r=5x10^{-4}$ to $5x10^{-3}$ μm. This interval contains about two thirds of the total EHPs, and the fit is best where the density is

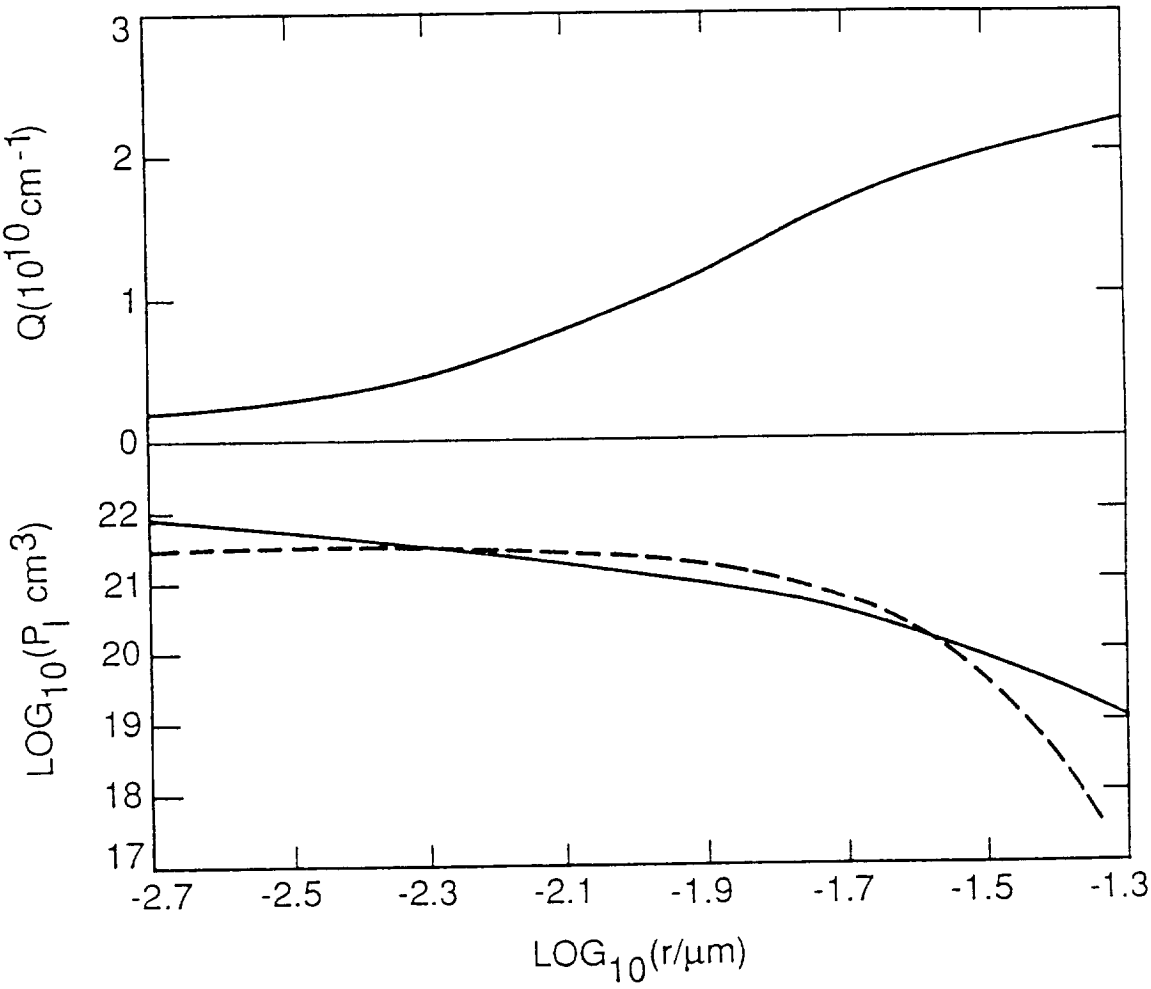

Figure 1. Radial distribution of initial track density: Produced by 270-MeV (incident energy) Kr after traveling 5 μm in Si. The lower solid curve is the volume density and the dashed curve is a fit to it. Upper solid curve is the total number of EHPs contained within the specified radius.

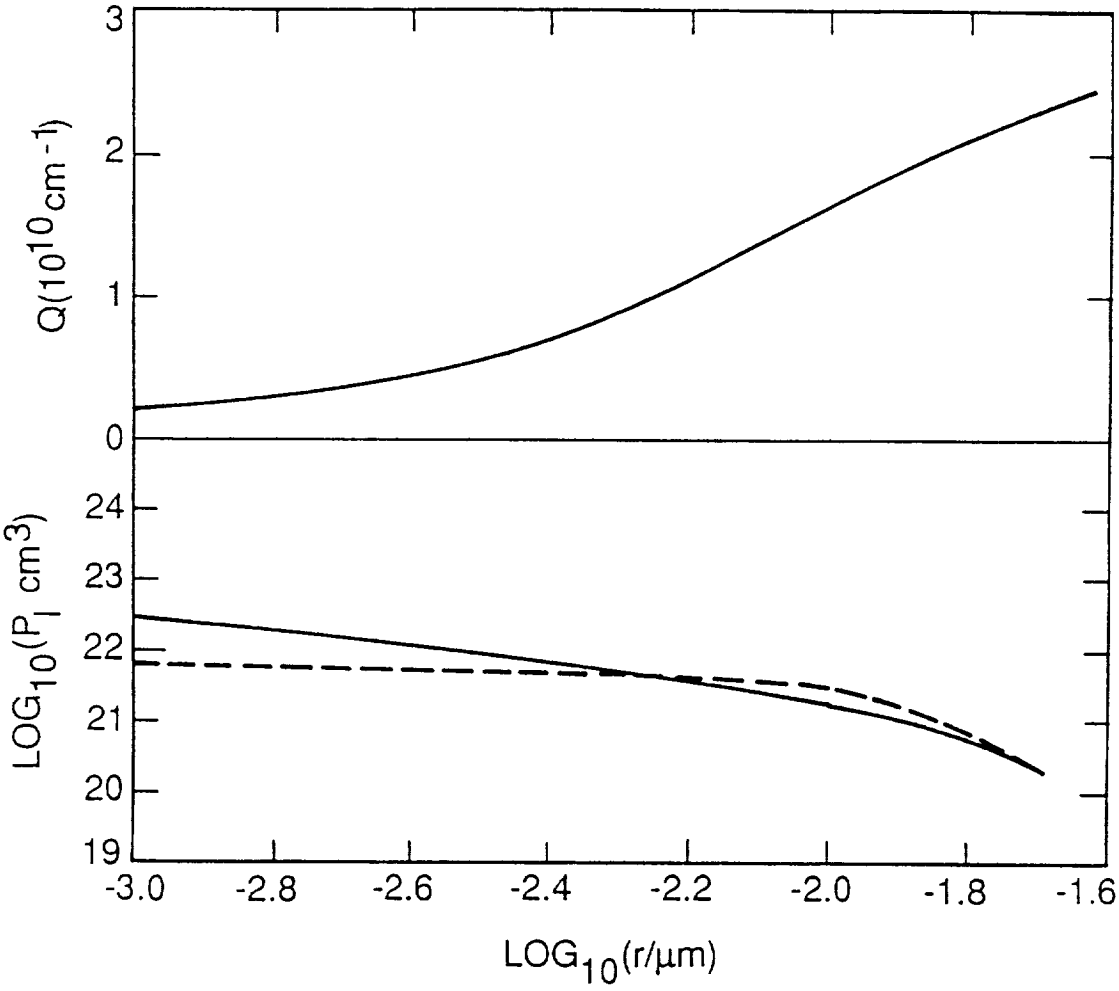

Figure 2. Radial distribution of initial track density: Same as Figure 1 except that the depth is 15 μm.

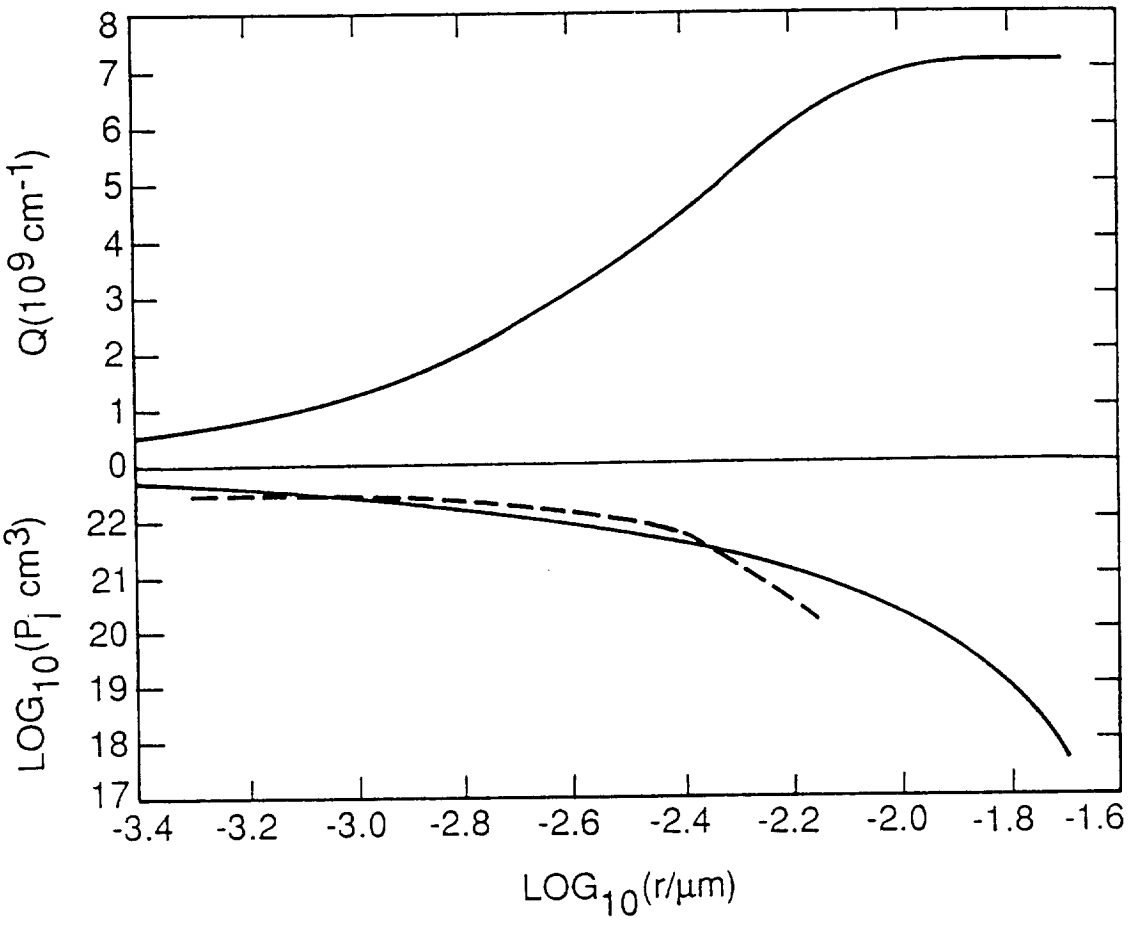

Figure 3. Radial distribution of initial track density: Same as Figure 1 except that the depth is 25 μm.

largest (with the exception of $r<5x10^{-4}$ μm, but less than 10% of the EHPs are located there) which is also where AR is most important.

The fitting curves in Figures 1, 2, and 3 are characterized by $r_c=1.5x10^{-2}$, $1.1x10^{-2}$, and $2.76x10^{-3}$ μm respectively, and $N_0=2.34x10^{10}$, $2.58x10^{10}$, and $7.2x10^{9}$ cm^{-1} respectively. Using these numbers, the computer code predicts the fractional losses to be 5.0%, 10.4%, and 12.3% respectively.

5. QUALITATIVE AND SEMI-QUANTITATIVE PREDICTIONS

It was shown in section 3 that the linear density approaches a non-zero limiting value as $t\rightarrow\infty$. This behavior is due to diffusion which lowers the EHP density and, therefore, the AR rate (if D was set equal to zero in (1), we would find that the linear density goes to zero). The AR rate decreases so fast with increasing t that some EHPs never will recombine (via AR) no matter how long we wait. It was also shown that the linear density is within approximately 2% of its asymptotic value after time T given by (38) (the word "approximately" is needed because it was the estimate P_{E1} rather than the actual P that was shown to be within 2% of its asymptotic value after time T). Using numbers from the examples of section 4, we find that T is on the order of a ps. This is very fast compared to most charge transport processes, including the recovery stage of funneling [with the possi-

ble exception of funneling in a very thin (less than 5 micron) epi-layer] [5]. AR is not fast compared to the collapse stage of funneling [5], but the section of track below the collapsed depletion region remains intact (it is not pulled apart by the electric field) immediately after the collapse. If the track is dense enough to cause a nearly complete collapse (so that nearly all of the track remains intact, which is the expected situation for tracks dense enough for AR to be important), the collapse stage will not significantly affect AR. Therefore, AR is expected to occur as section 3 predicted during a typical funneling process, and be essentially finished before any significant charge collection occurs. Therefore, when accompanying many charge transport processes, including funneling, AR should have the same effect as a reduction in ion linear energy transfer (LET). We can define another LET, which will be called the "reduced LET", which relates to surviving linear density in the same way that ordinary LET relates to initial linear density. Charge collection calculations should automatically include AR losses if reduced LET replaces ordinary LET. Single-event upset rate calculations should automatically include AR losses if experimentally measured device cross sections and Heinrich flux are plotted against reduced LET instead of ordinary LET.

If we agree to call a 5 to 10% loss of EHPs "marginally important", then the examples of section 4 predict that AR is of marginal importance for 270-MeV Kr and, therefore, of major importance for ions exhibiting a significantly larger loss.

6. SOURCES OF ERROR

There are a number of sources of error in these predictions of AR losses. The first is the replacement of a complicated system of nonlinear equations (the equations used by PISCES) with the simple diffusion equation (2). The second source of error is the fact that the computer code (Appendix C) produces an approximate, not exact, solution to (2). The PISCES code is not practical for parametric studies (because of large CPU time) but it can be run once to access the errors stated above. A cylindrical coordinate version of PISCES was run for the 15 μm example of section 4. PISCES predicted a 10.1% loss compared to our prediction of a 10.4% loss. Thus, it appears that the first two sources of error are not too serious.

A third source of error is the need to curve fit a function of the form (50) to the initial EHP density, which might look nothing like a Gaussian. The amount of error depends on the individual case, but can be estimated by trying several fits and running the code for each to determine how sensitive the predicted AR loss is to N_0 and r_c. The error might be reduced by an analysis (which remains to be worked out) that tells us how to select good values for N_0 and r_c.

The final source of error might be the most difficult to deal with. The equation used to solve for P assumes the charge carriers to be thermalized (an assumption also made by PISCES). But

significant AR requires r_c to be on the order of 10^{-3} or 10^{-2} μm and, under these conditions, some of the AR occurs in a tiny fraction of a picosecond. It is not clear how thermalized the track is during AR. The impact of this source of error is unknown at this time and quantitative estimates should be regarded as unreliable until they are supported by experimental measurements.

7. CONCLUSION

Quantitative estimates should be regarded as unreliable at this time, as stated in section 6, but it is reasonable to expect the qualitative statements, regarding the existence and use of reduced LET (see section 5), to be valid. Although unreliable, the quantitative estimates give credibility to the assertion that AR is of marginal importance to 270-MeV Kr tracks and of major importance to denser tracks. Therefore, it would be highly desirable to design and conduct an experiment that can directly measure reduced LET for Kr and heavier ions.

APPENDIX A

The objective is to show that iteration of (17) produces a sequence that converges to the solution P. It suffices to show that (17) satisfies the hypothesis of Banach's Fixed Point Theorem [6]. This will imply not only convergence but also that each iterate is at least as good of an approximation to P as the previous iterate.

Write (17) as

$$P = \underline{T}P \tag{A1}$$

where $\underline{T}$ is the operator defined by

$$\underline{T}P \equiv P_B + (4\pi D)^{-1}\int_0^t\int [BP - CF(P)]\, e^{-B(t-t')}G\, d^2X'\, dt'. \tag{A2}$$

We will work with the set of continuous functions and the maximum norm, which produces a complete metric space [7]. $\underline{T}$ is obviously a self mapping, i.e., it maps continuous functions into continuous functions. The only remaining condition that must be established is the existence of an $\alpha<1$ such that

$$||\underline{T}P_1-\underline{T}P_2|| \leq \alpha||P_1-P_2|| \tag{A3}$$

for all P_1 and P_2. $||*||$ denotes the maximum norm, i.e.,

$$||f|| = \max_{\substack{r\in[0,\infty) \\ t\in[0,T]}} |f(r,t)|$$

where T is the largest value of t that the solution is required to apply to. To establish (A3), note that

$$||\underline{T}P_1-\underline{T}P_2||=(4\pi D)^{-1}||\int_0^t\int [V(P_1)-V(P_2)]e^{-B(t-t')}G\ d^2X'\ dt'|| \quad (A4)$$

where

$$V(\tau) \equiv B\tau-CF(\tau) = 3CP_M^2\tau-CF(\tau) \ .$$

Note that V is continuous and its derivative is defined and continuous except at two isolated points ($\tau=\pm P_M$). Therefore,

$$V(P_1)-V(P_2) = \int_{P_2}^{P_1} V'(\tau)\ d\tau \ . \quad (A5)$$

Except at the two isolated points, V' is bounded by

$$V'(\tau) \leq 3CP_M^2 \ .$$

Combining this with (A5) and (A4) gives

$$||\underline{T}P_1-\underline{T}P_2|| \leq (4\pi D)^{-1}||\int_0^t\int 3CP_M^2|P_1-P_2|\ e^{-B(t-t')}G\ d^2X'\ dt'||$$

$$\leq 3CP_M^2(4\pi D)^{-1}||P_1-P_2||\ ||\int_0^t e^{-B(t-t')}\int G\ d^2X'\ dt'||. \quad (A6)$$

The integral can be evaluated with the result

$$\int_0^t e^{-B(t-t')}\int G\ d^2X'\ dt' = 4\pi D(3CP_M^2)^{-1}[1-e^{-Bt}]$$

so that

$$||\int_0^t e^{-B(t-t')}\int G\ d^2X'\ dt'|| = \max_{t\epsilon[0,T]}|4\pi D(3CP_M^2)^{-1}[1-e^{-Bt}]|$$

$$= 4\pi D(3CP_M^2)^{-1}[1-e^{-Bt}]$$

and (A6) becomes

$$||\underline{T}P_1-\underline{T}P_2|| \leq \alpha||P_1-P_2||$$

where

$$\alpha \equiv 1-e^{-BT}\ .$$

Since $\alpha<1$, the proof is complete.

APPENDIX B

The objective is to prove (24) and (25). These statements are special cases of the more general statement which follows. Let $\beta_1(X,t)$ and $\beta_2(X,t)$ be bounded and well behaved (in the sense that div grad β and $\delta\beta/\delta t$ exist) and let them satisfy

$$\beta_1(X,0) = \beta_2(X,0) = P_I(X) \quad . \tag{B1}$$

Define g_1 and g_2 by

$$g_i \equiv C\beta_i^3 - D \text{ div grad } \beta_i - \delta\beta_i/\delta t \quad \text{for } i = 1,2 \quad . \tag{B2}$$

The conclusion is that if $g_2(X,t) \geq g_1(X,t)$ for all X and for all $t>0$, then $\beta_2(X,t) \geq \beta_1(X,t)$ for all X and for all $t>0$.

To prove this statement, let β_B be a constant that is an upper bound for both $|\beta_1|$ and $|\beta_2|$. Define F^* by

$$F^*(\tau) \equiv \begin{cases} \tau^3 & \text{if } |\tau| \leq \beta_B \\ \beta_B^2 \tau & \text{if } |\tau| > \beta_B \end{cases} \tag{B3}$$

and write (B2) as

$$D \text{ div grad } \beta_i - \delta\beta_i/\delta t = CF^*(\beta_i) - g_i \tag{B4}$$

which can be inverted (see section 3) to give

$$\beta_i = P_B + (4\pi D)^{-1} \int_0^t \int [B\beta_i - CF^*(\beta_i) + g_i] e^{-B(t-t')} G \, d^2X' \, dt' \quad \text{(B5)}$$

where

$$B \equiv 3C\beta_B^2 \quad \text{(B6)}$$

and P_B satisfies (12) and (13), except that B is now given by (B6) instead of (7). The presence of g_i in (B5) does not affect the operators contraction mapping property and we conclude, from Appendix A, that (B5) can be solved by iteration, starting with any initial guess. For i=1,2, let $\beta_i^{(j)}$ (parentheses emphasize that j is a superscript, not an exponent) be defined by

$$\beta_i^{(0)} = 0 \quad \text{(B7a)}$$

$$\beta_i^{(j+1)} = P_B + (4\pi D)^{-1} \int_0^t \int [B\beta_i^{(j)} - CF^*(\beta_i^{(j)}) + g_i] e^{-B(t-t')} G \, d^2X' \, dt' \, . \quad \text{(B7b)}$$

Note that

$$\beta_i = \lim_{j \to \infty} \beta_i^{(j)} \, .$$

Therefore, to show that $\beta_2 \geq \beta_1$, it suffices to show that $\beta_2^{(j)} \geq \beta_1^{(j)}$ for all j=1,2,.... This can be shown by induction. From

$$g_2 \geq g_1 \tag{B8}$$

and (B7) we have $\beta_2^{(1)} \geq \beta_1^{(1)}$. Now assume that

$$\beta_2^{(j)} \geq \beta_1^{(j)} \ . \tag{B9}$$

It suffices to show that this implies

$$\beta_2^{(j+1)} \geq \beta_1^{(j+1)} \ . \tag{B10}$$

Note that $B\tau\text{-}CF^*(\tau)$ is an increasing function of τ and assumption (B9) implies

$$B\beta_2^{(j)}\text{-}CF^*(\beta_2^{(j)}) \geq B\beta_1^{(j)}\text{-}CF^*(\beta_1^{(j)}) \ .$$

Combining this result with (B8) and (B7) produces (B10) and completes the proof.

APPENDIX C

```
      PROGRAM RECOM
      PARAMETER(NT=201)
      DIMENSION T(0:NT),F(NT),F3(NT),S(NT)
      REAL K,N,N1(NT),N2(NT)
      COMMON T,F,K,T0
C  SET CONSTANTS.
      WRITE(*,*)'ENTER INITIAL LINEAR TRACK DENSITY (1/CM)'
      READ*,N
      WRITE(*,*)'ENTER INITIAL CHARACTERISTIC RADIUS (CM)'
      READ*,RC
      D=17.3
      C=3.79E-31
      PI4=12.56637
      PI4D=PI4*D
      T0=RC*RC/(4.0*D)
      K=0.7357589*C*N*N/(PI4D*PI4D)
C  CALL A SUBROUTINE TO CONSTRUCT THE TIME POINTS T(0),..,T(NT).
C  ALL DATA TRANSFER IS THROUGH THE COMMON BLOCK.
      CALL TIME
C  CALL A SUBROUTINE TO CONSTRUCT THE ARRAY F WHICH REPRESENTS
C  THE FUNCTION f BY THE RELATION F(J)=f(T(J)). ALL DATA TRANSFER
C  IS THROUGH THE COMMON BLOCK.
      CALL FUN
C  CONSTRUCT AN ARRAY TO REPRESENT N1(T) GIVEN BY EQ.(43) AND AN
C  ARRAY TO REPRESENT F3(T) GIVEN BY EQ.(47).
      DO 10 J=1,NT
      TJ=T(J)
      F1=SQRT(2.0*C*TJ)/(PI4D*(TJ+T0))
      F2=N*F1*F(J)
      W1=SQRT(1.0+F2*F2)
      W2=ALOG(F2+W1)
      N1(J)=W2/F1
      F3(J)=(W2-F2/W1)/(TJ*F1)
   10 CONTINUE
C  CONSTRUCT THE INTEGRAL IN (44). S(J) IS THE INTEGRAL EVALUATED
C  AT t=T(J). CONSTRUCT N2(J) FROM THE INTEGRAL.
      S(1)=F3(1)*T(1)
      N2(1)=N-0.5*S(1)
      DO 20 J=1,NT-1
      S(J+1)=0.5*(F3(J)+F3(J+1))*(T(J+1)-T(J))+S(J)
      N2(J+1)=N-0.5*S(J+1)
   20 CONTINUE
C  OUTPUT THE DATA.
      OPEN(UNIT=1,FILE='RCOM.OUT',STATUS='UNKNOWN')
      REWIND(1)
      WRITE(1,*)'N =',N
      WRITE(1,*)'RC=',RC
      WRITE(1,*)' '
      WRITE(1,*)' '
      WRITE(1,*)'  TIME (SEC)       FRACTIONAL SURVIVING E-H PAIRS'
      DO 30 J=1,NT
      AVG=0.5*(N1(J)+N2(J))/N
```

```
      ERROR=0.5*(N2(J)-N1(J))/N
      WRITE(1,40) T(J),AVG,'+ or -',ERROR
   30 CONTINUE
      CLOSE(1)
   40 FORMAT(E12.4,F16.3,A8,F6.3)
      END
C*********************************************************************
      SUBROUTINE TIME
      PARAMETER(NT=201)
      DIMENSION T(0:NT),F(NT)
      REAL K
      COMMON T,F,K,T0
C  SELECT POINTS ON THE TIME AXIS AND DENOTE THEM AS T(0),...T(NT),
C  WHERE T(0)=0, T(1)=T0/100, T(NT)=150K, AND THE REMAINING Ts
C  ARE CHOSEN SO THAT T(1),...,T(NT) ARE EQUALLY SPACED ON A
C  LOGARITHMIC SCALE.
      T(0)=0.0
      T(1)=T0/100.0
      T(NT)=150.0*K
      RNT=FLOAT(NT)
      A=ALOG10(T(NT)/T(1))/(RNT-1.0)
      B=ALOG10(T(1)/T0)-A
      DO 10 J=2,NT-1
      RJ=FLOAT(J)
      T(J)=T0*10.0**(A*RJ+B)
   10 CONTINUE
      RETURN
      END
C*********************************************************************
      SUBROUTINE FUN
      PARAMETER(NT=201)
      DIMENSION T(0:NT),F(NT),H1(NT),S(NT),F1(NT)
      REAL K
      COMMON T,F,K,T0
C  THE FUNCTION f IN EQ.(37) IS REPRESENTED BY THE ARRAY F AND IS
C  SOLVED BY ITERATION. FIRST CONSTRUCT THE INITIAL GUESS.
      DO 10 J=1,NT
      F(J)=1.0
   10 CONTINUE
C  START THE ITERATION LOOP.
   20 CONTINUE
C  CONSTRUCT ARRAYS TO SIMPLIFY THE INTEGRAL IN (37). H1 IS THE
C  INTEGRAND AND W IS THE ARGUMENT OF H. H IS A FUNCTION
C  SUBPROGRAM.
      DO 30 J=1,NT
      W=K*T(J)*F(J)*F(J)/(T(J)+T0)**2.0
      H1(J)=1.5*H(W)/(T(J)+T0)
   30 CONTINUE
C  CONSTRUCT THE INTEGRAL IN (37). S(J) IS THE INTEGRAL
C  EVALUATED AT T(J).
      S(1)=0.5*H1(1)*T(1)
      DO 40 J=1,NT-1
      S(J+1)=S(J)+0.5*(H1(J)+H1(J+1))*(T(J+1)-T(J))
   40 CONTINUE
C  STORE THE EXISTING Fs IN A NEW ARRAY, F1, FOR A FUTURE
```

```
C  ACCURACY CHECK, AND UPDATE THE VALUES STORED IN F USING (37).
       DO 50 J=1,NT
       F1(J)=F(J)
       F(J)=EXP(-1.0*S(J))
  50   CONTINUE
C   PERFORM ACCURACY CHECK AND ESCAPE FROM LOOP IF SATISFIED.
       IERROR=0
       DO 60 J=1,NT
       IF (ABS(F1(J)-F(J)).GE.0.0001) IERROR=1
  60   CONTINUE
       IF (IERROR.EQ.1) GO TO 20
       DO 70 J=1,NT
       F(J)=0.5*(F(J)+F1(J))
  70   CONTINUE
       RETURN
       END
C*****************************************************************
       FUNCTION H(X)
C  THE OBJECTIVE IS TO SOLVE FOR U=H(X). THIS IS DONE BY ITERATING
C  THE EQUATION U=0.5*(LN(X/U)+U) IF X >= .9 OR THE EQUATION
C  U=X*EXP(-U) IF X < .9. USE THE INITIAL GUESS U=X/2.
       U=0.5*X
  10   IF (X.GE.0.9) THEN
          U=0.5*(ALOG(X/U)+U)
          ELSE
          U=X*EXP(-U)
          END IF
       IF (ABS(U*EXP(U)/X-1.0).LE.0.0001) THEN
          H=U
          GO TO 20
          END IF
       GO TO 10
  20   CONTINUE
       RETURN
       END
```

REFERENCES

[1] J.A. Zoutendyk, L.S. Smith, and L.D. Edmonds, "Response of a DRAM to single-ion tracks of different heavy-ion species and stopping powers," IEEE Transactions on Nuclear Science, Vol. 37, No. 6, December 1990.

[2] M.R. Pinto, C.S. Rafferty, and R.W. Dutton, PISCES II: Poisson and Continuity Equation Solver, Stanford University, September 1984.

[3] P.M. Morse and H. Feshbach, Methods of Theoretical Physics, Part 1, McGraw-Hill, pp. 860-861, 1953.

[4] R.C. Martin, N.M. Ghoniem, Y. Song, and J.S. Cable, "The size effect of ion charge tracks on single event multiple-bit upset," IEEE Transactions on Nuclear Science, Vol. NS-34, No. 6, December 1987.

[5] L.D. Edmonds, "A simple estimate of funneling assisted charge collection," IEEE Transactions on Nuclear Science, Vol. 38, No. 2, April 1991.

[6] E. Kreyszig, Introductory Functional Analysis with Applications, Wiley, New York, p. 300, 1978.

[7] E. Kreyszig, Introductory Functional Analysis with Applications, Wiley, New York, p. 36, 1978.